Assault frequency and preformation probability of the alpha emission process

H.F. Zhang, G. Royer, J.Q. Li

On the assault frequency and preformation probability of the α emission process

H.F. Zhang

School of Nuclear Science and Technology, Lanzhou University, Lanzhou 730000, People's Republic of China

G. Royer

Laboratoire Subatech, UMR: IN2P3/CNRS-Université-Ecole des Mines, Nantes 44, France

J.Q. Li and W. Zuo

Institute of Modern Physics, Chinese Academy of Sciences, Lanzhou 730000, People's Republic of China

A study of the assault frequency and preformation factor of the α decay description is performed from the experimental α decay constant and the penetration probabilities calculated from the GLDM potential barriers. To determine the assault frequency a quantum mechanical method using an harmonic oscillator is introduced and lead to values of around $10^{21} s^{-1}$ similar to the ones calculated within the classical method. The preformation probability is around $10^{-1} - 10^{-2}$. The results for even-even Po isotopes are discussed for illustration. While the assault frequency presents only a shallow minimum in the vinicity of the magic neutron number 126 the preformation factor and mainly the penetrability probability diminish strongly around $N = 126$.

The α decay theory was firstly developed in 1928 [1, 2]. It describes the α radioactivity as a quantum tunneling through the potential barrier separating the mother nucleus energy and the total energy of the separated α particle and daughter nucleus. Later on, cluster-like [3–8] and fission-like [9–14] theories have been used to explain the α emission process. The decay constant λ is the product of three terms : the assault frequency ν, the barrier penetrability P and the α preformation probability P_α. Often the assault frequency is calculated supposing that the α particle moves classically back and forth inside the nucleus and is even sometimes taken as a constant. The cluster preformation probability corresponds rather to the penetrability of the part of the barrier before reaching the separation point while the barrier penetrability is rather associated with the external part of the barrier when the fragments are separated.

Firstly, the potential barrier governing the α particle emission has been determined within the generalized liquid drop model (GLDM) taking into account the mass and charge asymmetry [10, 14, 15]. The total energy is the sum of the volume, surface, Coulomb and proximity energies. When the nuclei are separated:

$$E_V = -15.494\left[(1-1.8I_1^2)A_1 + (1-1.8I_2^2)A_2\right] \text{ MeV}, \quad (1)$$

$$E_S = 17.9439\left[(1-2.6I_1^2)A_1^{2/3} + (1-2.6I_2^2)A_2^{2/3}\right] \text{ MeV}, \quad (2)$$

$$E_C = 0.6e^2Z_1^2/R_1 + 0.6e^2Z_2^2/R_2 + e^2Z_1Z_2/r, \quad (3)$$

where A_i, Z_i, R_i and I_i are the mass numbers, charge numbers, radii and relative neutron excesses of the two nuclei. r is the distance between the mass centres.

For one-body shapes, the surface and Coulomb energies are defined as:

$$E_S = 17.9439(1-2.6I^2)A^{2/3}(S/4\pi R_0^2) \text{ MeV}, \quad (4)$$

$$E_C = 0.6e^2(Z^2/R_0)\times 0.5\int (V(\theta)/V_0)(R(\theta)/R_0)^3 \sin\theta d\theta. \quad (5)$$

S is the surface of the one-body deformed nucleus. $V(\theta)$ is the electrostatic potential at the surface and V_0 the surface potential of the sphere.

When there are nucleons in regard in a neck or a gap between separated fragments a proximity energy must be added to take into account the effects of the nuclear forces between the close surfaces,

$$E_{\text{Prox}}(r) = 2\gamma\int_{h_{\min}}^{h_{\max}} \Phi\left[D(r,h)/b\right] 2\pi h dh. \quad (6)$$

h is the distance varying from the neck radius or zero to the height of the neck border. D is the distance between the surfaces in regard and $b = 0.99$ fm the surface width. Φ is the proximity function. The surface parameter γ is the geometric mean between the surface parameters of the two fragments. This term is essential to describe smoothly the one-body to two-body transition and to obtain reasonable potential barrier heights. It moves the barrier top to an external position and strongly decreases the pure Coulomb barrier. The experimental Q_α is taken into account. It has been previously shown that the combination of this GLDM and of a quasi-molecular shape sequence allows to reproduce the fusion barrier heights and radii, the fission, the α decay and the proton and cluster radioactivity data [10, 15–18].

The barrier penetrability P has been calculated within the action integral :

$$P = exp[-\frac{2}{\hbar}\int_{R_{\text{in}}}^{R_{\text{out}}} \sqrt{2B(r)(E(r)-E(sphere))}\, dr] . \quad (7)$$

Then the knowledge of the experimental decay constant λ and of the calculated barrier penetrability P allows to determine the behaviour of the product $P_\alpha \nu$ via the relation :

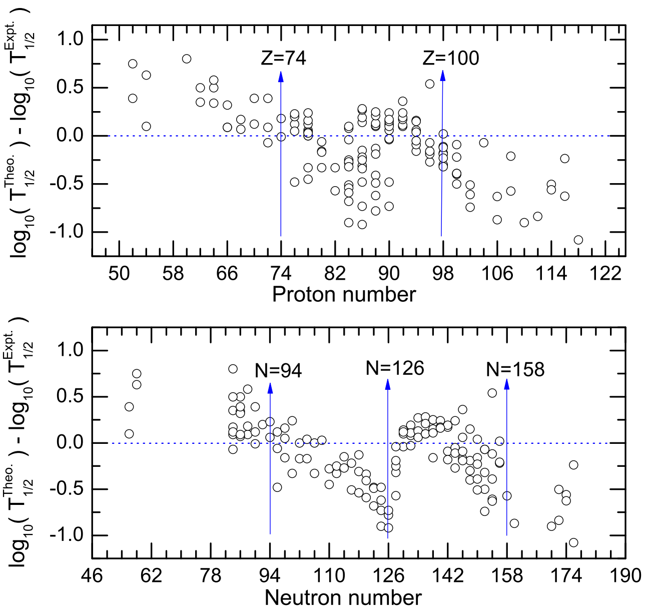

FIG. 1: The upper panel (lower panel) shows the deviations between calculated [10] and experimental α decay half lives for 131 even-even nuclei as a function of the proton number (neutron number).

$$\lambda = P_\alpha \nu \ P. \tag{8}$$

Let us first recall that in a previous study [10] the ratio λ/P has been fixed as 10^{20} s^{-1}. In Fig. 1, the deviation between the values of $\log_{10}[T_{1/2}(s)]$ within this approximation and the experimental ones is shown as functions of proton number (upper panel) and neutron number (lower panel). For the subset of the 131 even-even nuclei the root-mean-square deviation is 0.35. The theoretical data are slightly higher than the experimental ones for the lighter nuclei and systematically lower for the heaviest systems. When the proton number is under 74 (upper panel) or the neutron number is under 94 (lower panel), the calculations are higher than the experimental data, but for nuclei where the proton number is beyond 100 or the neutron number beyond 158 these theoretical predictions are lower than the experimental data. In addition, the deviations are larger when the proton number is about 82 and the neutron number is about 126. Some details on nuclear structure are missing when a fixed ratio λ/P is assumed.

In the present work, the empirical values of λ/P are extracted for 154 even-even nuclei. The experimental α decay half-lives are given in [19–22]. Fig. 2 displays a plot of $\log_{10} \lambda/P$ as a function of the neutron number. The values present a sharp decrease around the neutron magic number N=126 reconfirming this neutron closure shell structure. For a neutron number beyond about 155, the decreased trend appears again giving us some signals for an island of stability of superheavy nuclei. So this ratio is in reality slightly sensitive to the nuclear structure and can at least be used to detect shell effects.

As an example the extracted λ/P values are shown in the sixth column of the Tab. I for even-even Po isotopes. The range span from 10^{19} s^{-1} to more than 10^{20} s^{-1}.

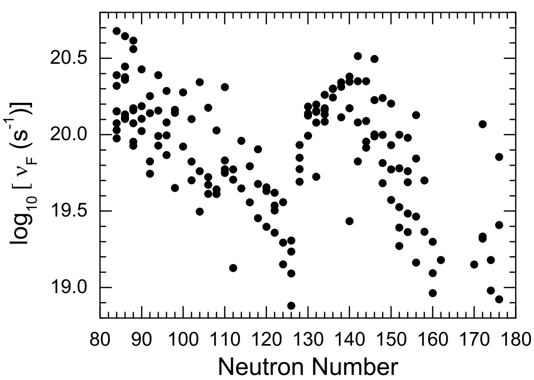

FIG. 2: $\log_{10} \lambda/P$ for 154 even-even nuclei versus the neutron number.

One way to determine the assault frequency is to imagine the α particle moving back and forth classically inside the nucleus with a velocity $v = \sqrt{\frac{2E_\alpha}{M}}$. Then it presents itself at the barrier with a frequency :

$$\nu_C = \left(\frac{1}{2R} \sqrt{\frac{2E_\alpha}{M}} \right) , \tag{9}$$

R being the radius of the parent nucleus, E_α the kinetic energy of the alpha particle, corrected for recoil and M its mass.

Then the preformation factor P_α of an α cluster inside the mother nucleus can be estimated using Eq.(8).

As an example, the calculated assault frequency ν from Eq.(9) as well as the preformation factor deduced from Eq.(8) and from the experimental constant decay are shown in the seventh and ninth columns of Tab. I respectively for the Po isotopes. The order of magnitude of ν is 10^{21} s^{-1}. Consequently, the preformation probability is of the order of $10^{-2} - 10^{-1}$. Both the penetration and preformation probabilities are reduced in the vicinity of the magic neutron number 126 but the penetration probability range is very large compared to that of the preformation factor. The penetration probability which is strongly connected to the Q_α value determines mainly the α decay half-life.

A new approach to deal with the assault frequency is proposed within a microscopic method deriving from the viewpoint of quantum mechanics. It assumes that the α particle which will be emitted vibrates nearby the surface of the parent nucleus in an harmonic oscillator potential

$V(r) = -V_0 + \frac{1}{2}\mu\omega^2 r^2$ with classical frequency ω and reduced mass μ. The virial theorem leads to

$$\mu\omega^2\overline{r^2} = (2n_r + \ell + \frac{3}{2})\hbar\omega, \quad (10)$$

where n_r and ℓ are the radial quantum number (corresponding to number of nodes) and angular momentum quantum number, respectively. $\sqrt{\overline{r^2}} =< \psi|r^2|\psi >^{1/2}$ is the rms radius of outermost α distributions in quantum mechanics. It equals the rms radius R_{n} of the parent nucleus. The assault frequency ν_M is related to the oscillation frequency ω by :

$$\nu_M = \frac{\omega}{2\pi} = \frac{(2n_r + \ell + \frac{3}{2})\hbar}{2\pi\mu R_{\mathrm{n}}^2} = \frac{(G + \frac{3}{2})\hbar}{1.2\pi\mu R^2}. \quad (11)$$

The relationship $R_n^2 = \frac{3}{5}R^2$ is used. The global quantum number $G = 2n_r + \ell$ of a cluster state is estimated by the Wildermuth rule [23] as

$$G = 2n + \ell = \sum_{i=1}^{4} g_i \ , \quad (12)$$

where n is the number of nodes of the α-core wave function; ℓ is the orbital angular momentum of the cluster motion; and g_i is the oscillator quantum number of a cluster nucleon. g_i equals 4 for nuclei with $(Z, N) \le 82$, $g_i = 5$ for $82 < (Z, N) \le 126$, and $g_i = 6$ for (Z,N)> 126, corresponding to the $4\hbar\omega$, $5\hbar\omega$, and $6\hbar\omega$ oscillator shells, respectively, where N and Z are the proton and neutron numbers of the parent nucleus (see also Ref. [24]). However, since a heavy nucleus involves usually mixed oscillator shells, the determination of the G value with the Wildermuth rule can be ambiguous to some extent, usually with an uncertainty of 2 or 4 in even-even heavy nuclei [25].

The estimated microscopic assault frequency from Eq.(11) is shown in the eighth column of the Tab.I and Fig. 3 for even-even Po isotopes. The order of magnitude of ν_M is 10^{21} s^{-1} same as that of ν_C which proves that the two calculations are consistent.

To study the correlation between the assault frequency and the structure properties, the values of $\nu/10^{21}s^{-1}$ for the even-even Po isotopes used within the classical approach and estimated by the microscopic method are shown as a function of the neutron number in the Fig. 4 respectively using triangles and black circles. The shapes of the two curves are similar and the values of ν_M from the microscopic calculations are always larger than ν_C used classically but never beyond two times implying again that the two different methods can be used. The assault frequency of the isotopes generally decreases with increasing neutron number up to the spherical shell closure N=126, where the minimum of the assault frequency occurs, and then they increase quickly with the neutron number. It is clear that the α assault frequencies against the potential barrier are sensitive to the nuclear shell closure effects.

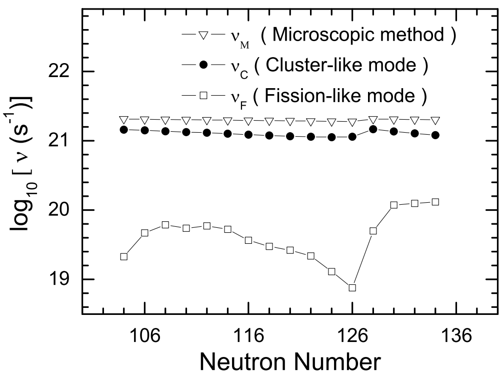

FIG. 3: $\log_{10}\nu$ for the even-even Po isotopes.

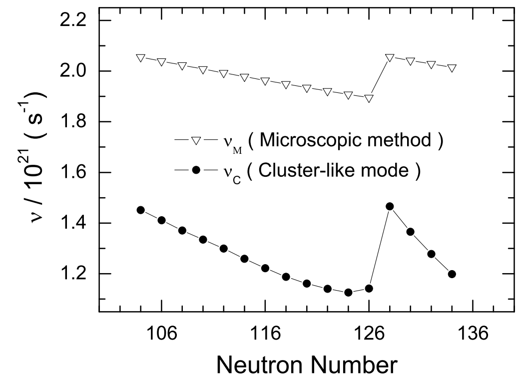

FIG. 4: $\nu/10^{21}$ for the even-even Po isotopes.

In conclusion, a study of the assault frequency and preformation factor of the α decay is performed from the experimental α decay constant and the penetration probabilities calculated from the WKB approximation and the GLDM potential barriers. The approximation of a constant value of λ/P is relatively rough. To determine the assault frequency a quantum mechanical method using an harmonic oscillator is introduced and lead to values of around $10^{21}s^{-1}$ similar to the ones calculated within the classical method using the picture of a particle moving back and forth inside the nucleus. Then the preformation probability is around $10^{-1} - 10^{-2}$. The results for even-even Po isotopes from ground-state to ground-state α emissions are discussed for illustration. While the assault frequency presents only a shallow minimum in the vinicity of the magic neutron number 126 the preformation factor and mainly the penetrability probability diminish strongly around $N = 126$. The small value of the preformation factor suggests that the α decay is rather a radioactive emission process of a cluster formed on the surface of the nucleus but before the potential barrier penetration.

TABLE I: Characteristics of the α decay for the even-even Po isotopes. The four first columns correspond respectively to the mother nucleus, the experimental Q_α, $\log_{10}[T_{1/2}(s)]$ and the experimental decay constant λ. The fifth column is the penetration probability. The three following columns give respectively the ratio λ/P the assault frequency obtained within the classical approach and using a quantum mechanical approach. The last column displays the preformation probability.

Nuclei	Q_α [MeV]	$\log_{10}[T_\alpha(s)]$	$\lambda[s^{-1}]$	P	$\lambda/P[s^{-1}]$	$\nu_C[s^{-1}]$	$\nu_M[s^{-1}]$	P_α
$^{188}_{84}$Po	8.087	-3.40	1.733×10^{3}	8.129×10^{-17}	2.133×10^{19}	1.451×10^{21}	2.055×10^{21}	0.0147
$^{190}_{84}$Po	7.693	-2.60	2.772×10^{2}	5.907×10^{-18}	4.698×10^{19}	1.411×10^{21}	2.039×10^{21}	0.0333
$^{192}_{84}$Po	7.319	-1.54	2.392×10^{1}	3.909×10^{-19}	6.119×10^{19}	1.371×10^{21}	2.023×10^{21}	0.0446
$^{194}_{84}$Po	6.990	-0.41	1.782×10^{0}	3.249×10^{-20}	5.485×10^{19}	1.335×10^{21}	2.008×10^{21}	0.0410
$^{196}_{84}$Po	6.660	0.76	1.205×10^{-1}	2.041×10^{-21}	5.904×10^{19}	1.299×10^{21}	1.993×10^{21}	0.0455
$^{198}_{84}$Po	6.310	2.18	4.580×10^{-3}	8.283×10^{-23}	5.529×10^{19}	1.259×10^{21}	1.978×10^{21}	0.0439
$^{200}_{84}$Po	5.980	3.79	1.124×10^{-4}	3.066×10^{-24}	3.666×10^{19}	1.222×10^{21}	1.963×10^{21}	0.0300
$^{202}_{84}$Po	5.700	5.13	5.138×10^{-6}	1.721×10^{-25}	2.985×10^{19}	1.188×10^{21}	1.949×10^{21}	0.0251
$^{204}_{84}$Po	5.480	6.28	3.638×10^{-7}	1.376×10^{-26}	2.644×10^{19}	1.161×10^{21}	1.935×10^{21}	0.0228
$^{206}_{84}$Po	5.330	7.15	4.907×10^{-8}	2.254×10^{-27}	2.177×10^{19}	1.141×10^{21}	1.921×10^{21}	0.0191
$^{208}_{84}$Po	5.220	7.97	7.427×10^{-9}	5.727×10^{-28}	1.297×10^{19}	1.126×10^{21}	1.908×10^{21}	0.0115
$^{210}_{84}$Po	5.407	7.08	5.765×10^{-8}	7.615×10^{-27}	0.757×10^{19}	1.142×10^{21}	1.895×10^{21}	0.0065
$^{212}_{84}$Po	8.950	-6.52	2.295×10^{6}	4.598×10^{-14}	4.991×10^{19}	1.466×10^{21}	2.056×10^{21}	0.0341
$^{214}_{84}$Po	7.830	-3.87	5.138×10^{3}	4.309×10^{-17}	1.187×10^{20}	1.366×10^{21}	2.042×10^{21}	0.0873
$^{216}_{84}$Po	6.900	-0.82	4.580×10^{0}	3.670×10^{-20}	1.248×10^{20}	1.278×10^{21}	2.028×10^{21}	0.0976
$^{218}_{84}$Po	6.110	2.27	3.722×10^{-3}	2.844×10^{-23}	1.309×10^{20}	1.199×10^{21}	2.015×10^{21}	0.1092

I. ACKNOWLEDGEMENTS

The work was supported by the National Natural Science Foundation of China (10775061,10975064,10875152, 10875151, and 10740420550); the Fundamental Research Fund for Physics and Mathematics of Lanzhou University (grants LZULL200805), the Fundamental Research Funds for the Central Universities (grants lzujbky-2009-21); by the CAS Knowledge Innovation Project NO.KJCX-SYW-N02; The Major State Basic Research Developing Program of China (2007CB815004).

[1] G. Gamov, Z. Phys. **51**, (1928) 204 .
[2] E. U. Condon and R. W. Gurney, Nature **122**, (1928) 439 .
[3] S.S. Malik and R. K. Gupta, Phys. Rev. **C 39**, (1989) 1992.
[4] A. Ludu, A. Sandulescu, and W. Greiner, Int. J. Mod. Phys. **E 1**, (1992) 169.
[5] C. Xu and Z.Z. Ren, Phys. Rev. **C 74**, (2006) 014304.
[6] J.C. Pei, F.R. Xu, Z.J. Lin, and E.G. Zhao, Phys. Rev. **C 76**, (2007) 044326.
[7] G. L. Zhang, X. Y. Le, and H. Q. Zhang, Nucl. Phys. **A 823**, (2009) 16.
[8] Tiekuang Dong, and Zhongzhou Ren, Phys. Rev. **C 82**, (2010) 034320.
[9] D. N. Poenaru,M. Ivascu, A. Sandulescu, and W. Greiner, Phys. Rev. **C 32**, (1985) 572 ; D.N. Poenaru, I.H. Plonski, and W. Greiner, Phys. Rev. **C 74**, (2006) 014312.
[10] G. Royer, J. Phys. **G** : Nucl. Part. Phys. **26**, (2000) 1149 .
[11] D. N. Basu, and C. Samanta, Phys. Rev. **C 75** (2007) 047306.
[12] V.Yu. Denisov, A.A. Khudenko, At. Data Nucl. Data Tables **95**, (2009) 815.
[13] G. Royer and H.F. Zhang, Phys. Rev. C **77**, (2008) 037602.
[14] G. Royer, Nucl. Phys. **A 848**, (2010) 279.
[15] H.F. Zhang, W. Zuo, J.Q. Li, and G. Royer, Phys. Rev. **C 74**, (2006) 017304.
[16] H.F. Zhang and G. Royer, Phys. Rev. **C 77**, (2008) 054318.
[17] G. Royer and B. Remaud, Nucl. Phys. **A 444**, (1985) 477.
[18] Y.Z. Wang, H.F. Zhang, J.M. Dong, G. Royer, Phys. Rev. **C 79** (2009) 014316.
[19] G. Audi, O. Bersillon, J. Blachot, and A.H. Wapstra, Nucl. Phys. **A 729**, (2003) 3.
[20] J. Dvorak *et al.*, Phys. Rev. Lett **97**, (2006) 242501.
[21] S. Hofmann, G. Münzenberg, Rev. Mod. Phys. **72**, (2000) 733; S. Hofmann *et al.*, Eur. Phys. J. **A 32**, (2007) 251.
[22] Yu.Ts. Oganessian *et al.*, Phys. Rev. **C 63**, (2000) 011301(R); Phys. Rev. **C 70**, (2004) 064609; Phys. Rev. **C 72**, (2005) 034611; Phys. Rev. **C 74**, (2006) 044602; Phys. Rev. **C 76**, (2007) 011601(R).
[23] K. Wildermuth and Y.C. Tang, A Unified Theory of the Nucleus (Academic Press, New York, 1977).
[24] P. Mohr, Phys. Rev. **C 61**, (2000) 045802.
[25] B. Buck, A.C. Merchant, and S.M. Perez, Phys. Rev. **51**, (1995) 559.